Al-Mustansiriyah Journal of Science
ISSN: 1814-635X (print), ISSN:2521-3520 (online) Volume 34, Issue 2, 2023 DOI: http://doi.org/10.23851/mjs.v34i2.1223

Research Article **Open Access**

Influence Study of Etching Time for Porous Silicon on Morphological, Optical, Electrical and Spectral Responsivity Properties

Aliyaa A. Urabe[1*], Uday M. Nayef[2], Randa Kamel[1]

[1]Department of Physics, College of Science, Mustansiriyah University, 10052 Baghdad, IRAQ.
[2] Department of Applied Science, University of Technology, 10066 Baghdad, IRAQ.

[*]Correspondent contact: aliyaa88abdullah@uomustansiriyah.edu.iq
https://orcid.org/0009-0009-9244-3856

Article Info

Received
14/09/2022

Accepted
31/01/2023

Published
30/06/2023

ABSTRACT

In this investigation, n-type (100) silicon wafers with a thickness of 600 ± 25 μm and resistance of 0.1-100 μΩ were used to manufacture porous silicon. With the aid of hydrofluoric acid (HF) with a 20% concentration, a current density of 20 mA/cm^2, and various experimental drilling times of 5, 15, and 25 minutes with the fixation of other parameters, the photoelectrochemical etching method was successful. The morphology of porous silicon was investigated using scanning electron microscopy (SEM), the XRD- diffraction wide of porous silicon creation with rising apex peaks was confirmed, and (AFM) sponge-like morphology was seen, and the pore diameter grew larger as drilling time rose. In a drilling time of 15 minutes, it is able to quantify both the vibrational and electrical characteristics of the energy band gap using Raman analysis and PL detection. Investigate sample samples' current voltage readings (J-V) at various etching times. Additionally, we discovered devices with a broad wavelength that react to the response in the investigation of the spectrum response PS AL/PS/SI/Al as a photodetector.

KEYWORDS: Porous silicon; PECE; etching time; photodetectors.

الخلاصة

في هذا البحث، تم استخدام رقائق السيليكون من من النوع n (100) بسماكة ٦٠٠ ± ٢٥ ميكرومتر مع المقاومة من ٠,١- ١٠٠ ميكرواوم لتصنيع السيليكون المسامي. بمساعدة حمض الهيدروفلوريك (HF) بتركيز ٢٠٪، وكثافة تيار تبلغ ٢٠ مللي أمبير/سم٢ ، وأوقات حفر تجريبية مختلفة تبلغ ٥ و ١٥ و ٢٥ دقيقة مع تثبيت معلمات أخرى ، كانت طريقة النقش الكهروكيميائية الضوئية ناجحة. تم التحقيق في مورفولوجيا السيليكون المسامي باستخدام المجهر الإلكتروني الماسح (SEM)، وتم تأكيد حيود XRD الواسع لإنشاء السيليكون المسامي مع ارتفاع قمم القمة، وشوهد (AFM) مورفولوجيا تشبه الإسفنج، ونما قطر المسام أكبر مع ارتفاع وقت الحفر. في وقت حفر مدته ١٥ دقيقة، إنه قادر على تحديد كل من الخصائص الاهتزازية والكهربائية لفجوة نطاق الطاقة باستخدام تحليل Raman واكتشاف PL. تحقق من قراءات الجهد الحالي لعينات العينات (J-V) في أوقات الحفر المختلفة. بالإضافة إلى ذلك، اكتشفنا أجهزة ذات طول موجي واسع تتفاعل مع الاستجابة في التحقيق في استجابة الطيف PS AL/PS /SI/Al ككاشف ضوئي.

INTRODUCTION

Generally, the Porous Silicon (PS) is one of the favorable materials because of its reactive internal surface and is very large. So, it has a high sensitivity to chemical and physical properties [1-4]. An inexpensive and simple invention, possessing the properties of ideal optoelectronics, it could be a basic base for depositing multiple nanomaterials, increasing the range of possible applications of PS in optics and integrated photonics [5-8]. PS is special material; therefore, it attracts the attention of many researchers for developing devices of optoelectronic and Photoconvergen [9-12]. Numerous techniques exist to create porous silicon, but the photoelectrochemical etching technique combines two techniques (photochemical and electrochemical). One of the most straightforward and trustworthy methods for creating PS is to use etching operations to create pores on a silicon substrate n or p types [12-16]. The properties of PS layers are strongly concerning to its morphology and topography, and control of the structure by extreme interest was specific,

topography and morphology of PS surface by variation the electrochemical etching parameters [16-17. Additionally, etching length is a significant factor that influences how the anodized PS's surface morphology [18-24]. Numerous earlier studies of the PS physical properties under a various range of parameters for the production of electrochemical etching have been carried out [25-30]. The relationship between PS morphology and fabrication circumstances employing photo- or electrochemical etching for silicon (n or p) type was investigated [31-34]. applied 10, 20, and 30 min. as etching times in order to crystalline silicon n-type (111) and (100) wafers in order to electrochemically etch PS [35-38]. It was confirmed that, while utilizing the electrochemical etching technique, the PS's depth, width, and roughness increased as the etching time rose [39-44]. Study behavior PS surface crack and nanostructure with the relationship between According to the parameters of the etching, such as the HF concentration, current density, or the type and level of the substrate doping [45-50], This work was prepared for porous silicon by the embossing method photo-electrochemical etching (PEC) by changing the engraving time while keeping the rest of the parameters constant and studying the effect of changing the engraving time on surface morphology, changing the pore size and clarifying the optical properties on the silicon nanolayer.

MATERIALS AND METHODS

Using n-type wafer phase orientation (100) silicon with a thickness of 600± 25µm and a resistivity of 0.1-100 Ω.cm, The PS was made employing the photo-electrochemical etching method (as shown in Figure 1) using high purity Hydrofluoric acid (Spanish industry/European Union) and diluting it with ethanol C_2H_5OH (99.9%) high purity to obtain a concentration of 20% in the rate of (41.66:58.34) to get a consistent etching and reduce hydrogen bubbles in the presence of a Teflon cell (non-reactive with HF) with a 20 mA/cm^2 current density Si wafer connects the cathode electrode to the anode electrode and vice versa. This process can be called anodizing. The last step is rinsing the sample with pentane to reduce the surface tension of the sample and to avoid cracks, and then with ethanol to get rid of the remnants of the electrolyte solution.

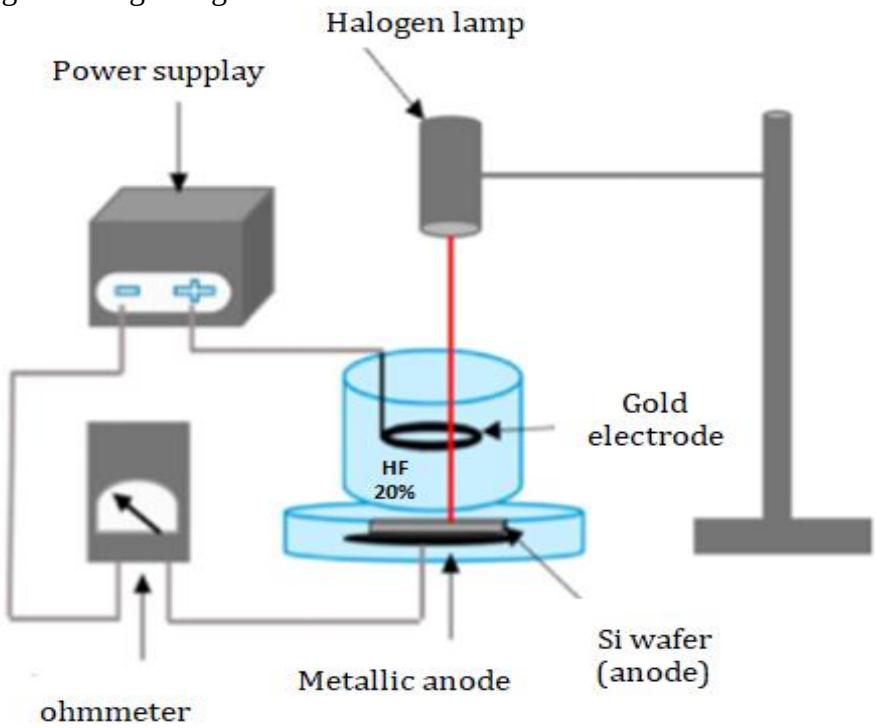

Figure 1. PS of the photo-electrochemical etches technique schematic shape.

RESULTS AND DISCUSSION

Figure 2a of the X-ray diffraction shows a sharp peak plane-oriented wafer (100) can be observed located at (2Θ = 69.44º) reflecting the cubic structure of the Si n-type (according to JCPDS No.27-1402). PS in Figure 2b shows XRD diffraction by an anodizing process in a current density is 20 mA/cm^2 and 15 min. etching time and a 20% HF concentration. The presence of a

ISSN: 1814-635X (print), ISSN:2521-3520 (online) Volume 34, Issue 2, 2023 DOI: http://doi.org/10.23851/mjs.v34i2.1223

splitting and widening peak around an angle of 69.9^{o} it having the same direction may be attributed to these increases in intensity leading to the crystallization of the silicon wafer after etching towards the size of the nanocrystal. However, etched porous silicon still has a single crystal structure even after etching, which results in a rightward displacement of the PS peak. PS has a smaller crystalline size than the c-Si peak, yet its diffraction angle is modest. (According to Scherer's formula).

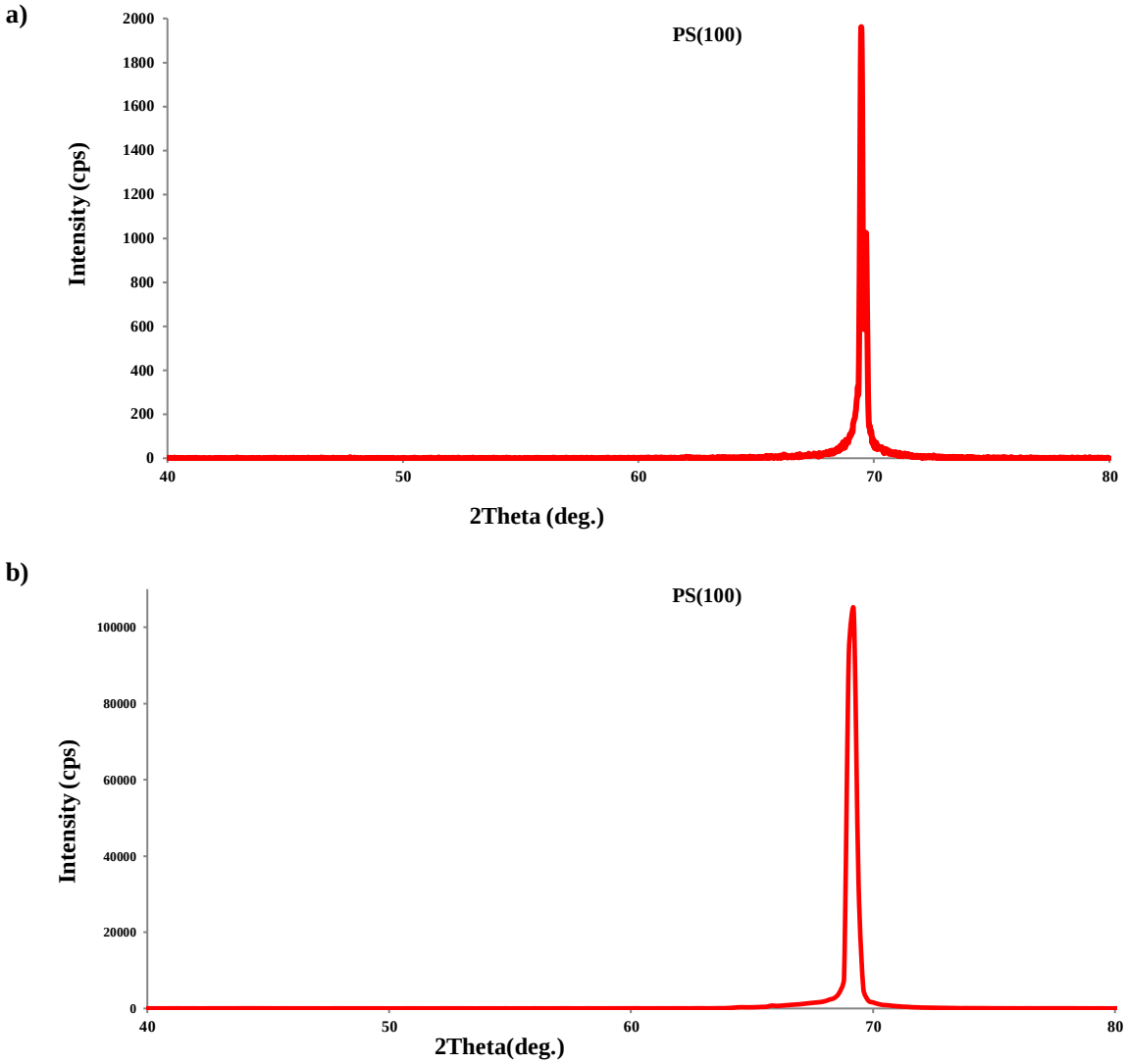

Figure 2. a) XRD pattern Si wafer prior to etching, b) XRD pattern of porous silicon following etching time 15 mint by HF_c= 20% and 20 mA/cm^2 current density.

Figure 3 shows the difference between the influence of etching time on the surface morphology and structure of silicon layers produced on silicon substrates using porous silicon for a period of 5, 15, and 25 min. from the time of etching using the image of SEM. Unlike grain agglomeration from porous silicon formation effect of engraving time during etching, SEM shows that the surface of the PS was etched in the entirety, and pores increased with increasing time for etching. As shown in Figures 3b, c the pores diameter increased over time, and the holes circular shape altered to a random one. This important change did not occur directly, but was the result of a transitional phase in which the sub-walls began to melt (overlap pores). Moreover, we enhanced the silicon dissolution process as a result of the disintegration of the thin walls with an increase in etching time.

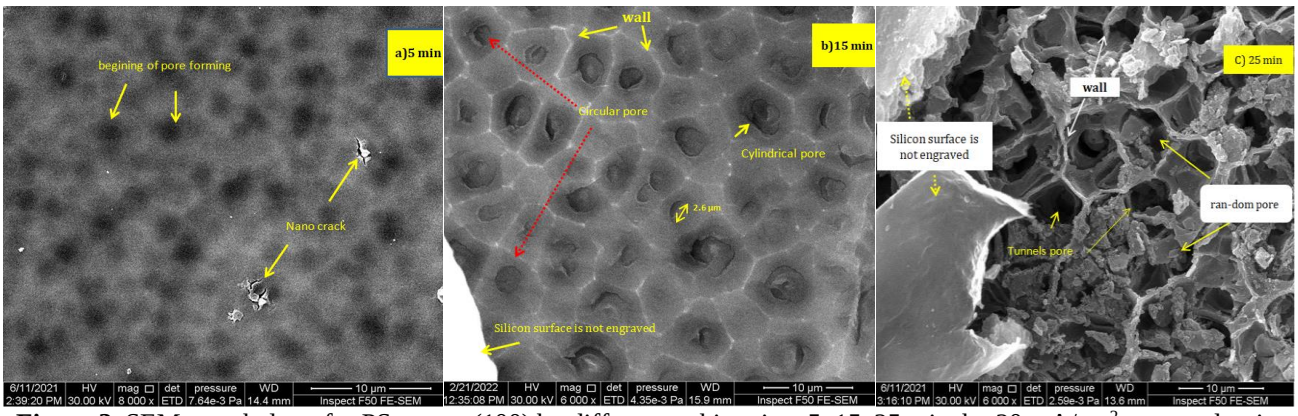

Figure 3. SEM morphology for PS n-type (100) by different etching time 5, 15, 25 min, by 20 mA/cm^2 current density and HF$_c$= 20 %.

Figure 4 shows the optical properties of PS using a photoluminescence spectrometer (PL) For three different drilling times are (5,15,25) minutes, we noticed the highest density 648, 635, 627 nm respectively these sharp peaks within the blue region of the electromagnetic spectrum are accompanied by an increase in the energy gap 1.91, 1.95, 2 eV successively nd that the PL density of PS is high at this limit of patterning within pours silicon nanocrystals. Recombination of the electron-hole pairs by the effects of the increase of the energy band gap and intensity, which enhances the reduction of the crystal size of PS wafer. This is consistent with SEM images showing different nano-wall sizes.

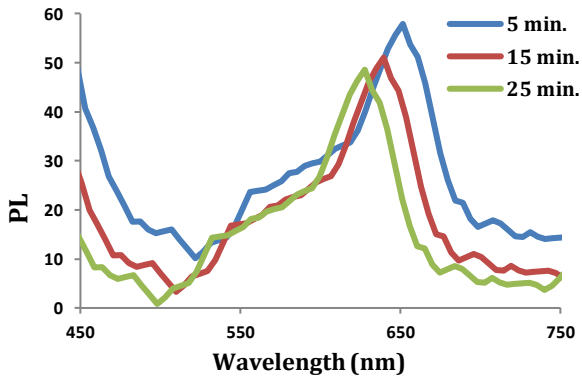

Figure 4. PL PS n-type by different etching time, by current density 20 mA/cm^2 and HF$_c$= 20 %.

Figure 5 displays the Raman spectrum of a porous silicon substrate under the condition of preparation HF$_c$= 20%, J= 20 mA/cm^2 current density and 15 min; the nanostructure PS layer is responsible for the strong peak at 521 cm^{-1}, whereas crystalline silicon (c-Si) Raman frequency is 520 cm^{-1}. This indicates that the PS was penetrated by light at 625 nm in order to reach the c-Si substrate. The peak at 1035 cm^{-1} represented the transversal photon propagating; the peaks at 1262 and 1527 cm^{-1} may be caused by shifting Si-H stretching vibrations.

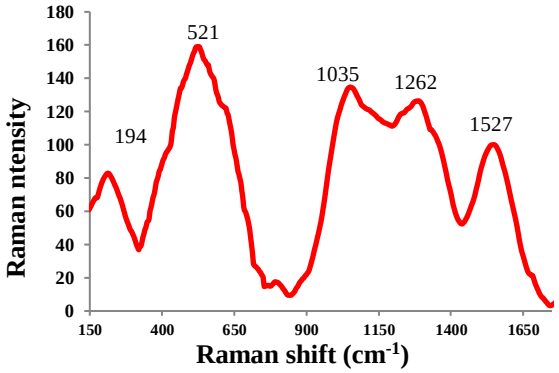

Figure 5. Raman of PS n-type by etching time 15 min, by current density 20 mA/cm^2 and HF$_c$= 20 %.

J-V characterization clarified in dark was practically measured in direction of forward and reverse bias from -5 to +5 V for PS layers at different etching times. Figure 6 shows 3 curves of current Al/PS/n-Si/Al under the influence of etching time because it affects PS nano-walls. With an increase in time, the resistance of PS increases due to the direct energy band gap. We see decrees current for forward and reverse voltage at the highest etching time due to the resistance increases due to the large energy band gap due to the decrease in the size (nano-walls as shown in SEM images) the effect of quantum confinement suggests that the etching time should increase. The energy band gap widens with decreased size. With incoming power densities of 5, 20, 60, and 125 mW/cm^2 photocurrent can produce electron-hole pairs in the depletion area due to its growing light current density as in Figure 6.

In this Figure, the three curves show a decrease in the luminous current when increasing etching time, this corresponds to an increase in the

porosity of the silicon wafer, and this enhances the responsiveness of the junction that was created between PS and n-Si. The value of photocurrent is higher than the dark current, but the decrease in Photocurrent with increasing etching time is shown in Figure 6 for the same reason above. Table 1 shows the ideality factor and barrier height based on the following equation, PS layer structure ΦB may be examined from J-V calculation [51].

$$n = \frac{q}{K_B T}\frac{dV}{d(\ln J)} \quad (1)$$

$$\Phi B = \frac{K_B T}{q}\ln\left(\frac{A^{**}T^2}{J}\right) \quad (2)$$

Denote V represents applied voltage, (K_B=1.38 x 10^{-23}J/K) Boltzmann constant, A^{**}(112 for the n-type Si) represents Richardson constant (A/cm^2 K^2), and J denotes the forward current density (μA/cm^2) [52].

Table 1. The height of the barrier, Value of ideality factor and the Saturation current for the sample PS at a varied prepared time of Sample.

Sample PS	Js (μA/cm^2)	n	Φ_Bx10^{-4} (eV)
5 min.	1.5	5.8	0.686
15 min.	1.3	5.37	0.688
25 min.	1.1	5.56	0.693

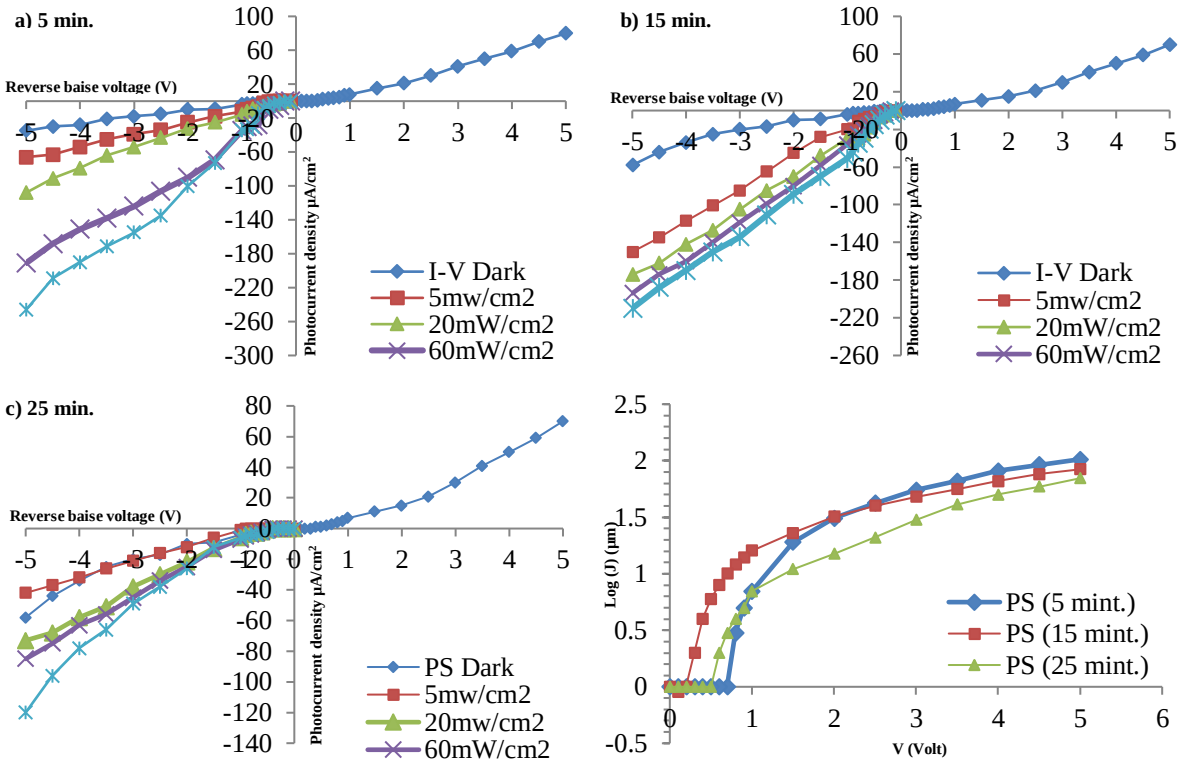

Figure 6. J_{ph}–V characterization of Al/n-S/PS by different etching time (a) 5 min. (b), 15min., (c) 25 min, by current density 20 mA/cm^2 and HF_c= 20 %.

Figure 7 shows the spectral responsivity of the Al/PS/n-Si/Al photoelectric detector after working with PS at different etching times of 5, 15, and 25 minutes, respectively, in the range of 400-900 nm at the bias of 2 Volts. Changing the response or spectral sensitivity is very important to determine the performance of the detector. Responsivity (R_λ) is the ratio between photocurrent products (I_{ph}) to the power light incident (P_{in}) increase in R_λ was evident with the increase in etching time, and the peaks were relatively consistent, the first at 600 nm for PS and the second region at 850 nm for Si (due to native oxide on the Si layer), the highest R_λ of the photo-detector device compared to other detectors PS were manufactured in a short time. This enhances distinctive the distinctive applied properties of Si due to the quantum confinement effect.

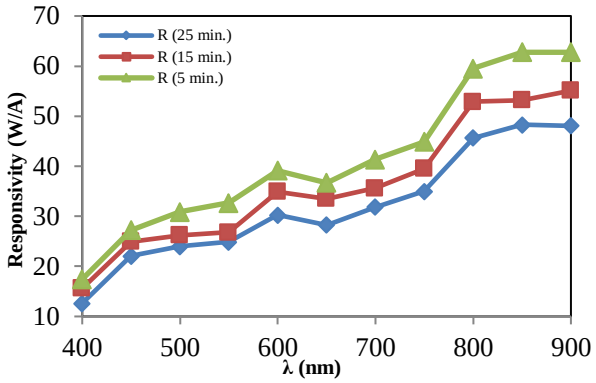

Figure 7. The Spectral responsiveness of Al/n-Si/PS/Al under various etching times 5, 15, and 25 min., with a current density of 20 mA/cm^2 and HF_c= 20 %.

CONCLUSIONS

In this work, a silicon matrix was manufactured in a way (PEC) with a different etching time, Between X-ray diffraction an increase in the intensity of the sharp peak of monocrystalline silicon with the same orientation, explained the morphology of the surface SEM the formation of larger pores accompanied by an increase in the energy gap with a decrease in wavelength (PL) These characteristics enabled us to manufacture a detector with a distinct spectral response that increases with increasing engraving time and an ideal factor that increases with a decreasing saturation current that enables us to obtain a photodetector in the least time, easiest and fastest Preparatory method.

ACKNOWLEDGMENTS

I would like to thank my mother university (Al-Mustansiriyah University / Faculty of Science) and thank you for the cooperation of the University of Technology.

Disclosure and Conflict of Interest: The authors declare that they have no conflicts of interest.

REFERENCE

[1] U. Nayef, M. Muayad, H. Khalaf, ZnO/PS/p-Si heterojunction properties. Eur. Phys. J. Appl. Phys. (2014). https://doi.org/10.1051/epjap/2014130470

[2] U. Nayef, Improve the efficiency of UV-detector by modifying the Si and porous silicon substrate with ZnS thin films. Optik 130, 441-447 (2017). https://doi.org/10.1016/j.ijleo.2016.10.077

[3] U. Nayef and I. Khudhair, Study of porous silicon humidity sensor vapors by photoluminescence quenching for organic solvents. Optik 135, 169-173 (2017). https://doi.org/10.1016/j.ijleo.2017.01.060

[4] U. Nayef, H. Hussein and A. Abdul Hussien, Study of photoluminescence quenching in porous silicon layers that using for chemical solvents vapor sensor. Optik 172, 1134-1139 (2018). https://doi.org/10.1016/j.ijleo.2018.07.112

[5] D. Buttard, D. Bellet, G. Dolino, ″Epitaxial growth of germanium dots on Si (001) surface covered by a very thin silicon oxide layer″, Journal of Applied Physics 83 (1998), pp. 5814-5822. https://doi.org/10.1063/1.367438

[6] Uday M. Nayef, Mohammed W. Muayad, and Haider A. Khalaf, Eur. Phys. J. Appl. Phys. (2014) 66: 20104. https://doi.org/10.1051/epjap/2014130470

[7] Jwar , Ahmad J., Uday M. Nayef, and Falah AH Mutlak. "Study effect of magnetic field on Au-TiO2 nanoparticles ablated on silicon nanostructures for gas sensors." Journal of Optics (2022): 1-9. https://doi.org/10.1007/s12596-022-00987-w

[8] U. Nayef, I. Khudhair, Synthesis of gold nanoparticles chemically doped with porous silicon for organic vapor sensor by using photoluminescence. Optik 154, 398-404 (2018). https://doi.org/10.1016/j.ijleo.2017.10.061

[9] H. Hussein, U. Nayef, A. Abdul Hussien, Synthesis of grapheme on porous silicon for vapor organic sensor by using photoluminescence. Optik 180, 61-70 (2019). https://doi.org/10.1016/j.ijleo.2018.10.222

[10] N. Abdulkhaleqa, A. Hasan, U. Nayef, Enhancement of photodetectors devices for silicon nanostructure from study effect of etching time by photoelectrochemical etching Technique. Optik 206, 164325 (2020). https://doi.org/10.1016/j.ijleo.2020.164325

[11] N. Abdulkhaleq, U. Nayef, A. Albarazanchi, MgO nanoparticles synthesis via laser ablation stationed on porous silicon for photoconversion application. Optik 212, 164793 (2020). https://doi.org/10.1016/j.ijleo.2020.164793

[12] U. Nayef, R. Kamel, Bi2O3 nanoparticles ablated on porous silicon for sensing NO2 gas. Optik 208, 164146 (2020). https://doi.org/10.1016/j.ijleo.2019.164146

[13] D. Jwied, U. Nayef, F. Mutlak, Preparation and characterization of C: Se nano-rods ablated on porous silicon. Optik 239, 166811 (2021). https://doi.org/10.1016/j.ijleo.2021.166811

[14] Alwan, A.M., A.A. Yousif, and L.A. Wali, A study on the morphology of the silver nanoparticles deposited on the n-type porous silicon prepared under different illumination types. Plasmonics, 2018. 13(4): p. 1191-1199. https://doi.org/10.1007/s11468-017-0620-3

[15] Chen, C., Song,Z., Chuanxiao., Achieving a high open-circuit voltage in inverted wide-bandgap perovskite solar cells with a graded perovskite homojunction. Nano Energy, 2019. 61: p. 141-147. https://doi.org/10.1016/j.nanoen.2019.04.069

[16] Suri, M., et al., Enhanced Open-Circuit Voltage of Wide-Bandgap Perovskite Photovoltaics by Using Alloyed (FA1-x Cs x) Pb (I1-x Br x) 3 Quantum Dots. ACS Energy Letters, 2019. 4(8): p. 1954-1960. https://doi.org/10.1021/acsenergylett.9b01030

[17] Alwan, A.M., I.A. Naseef, and A.B. Dheyab, Well controlling of plasmonic features of gold nanoparticles on macro porous silicon substrate by HF acid concentration. Plasmonics, 2018. 13(6): p. 2037-2045. https://doi.org/10.1007/s11468-018-0720-8

[18] Jansen, D., Naber,Ch., Ectors, D. Z. Lu, X.-M. Kong, F., The early hydration of OPC investigated by in-situ XRD, heat flow calorimetry, pore water analysis and 1H NMR: Learning about adsorbed ions from a complete mass balance approach. Cement and Concrete Research, 2018. 109: p. 230- 242. https://doi.org/10.1016/j.cemconres.2018.04.017

[19] Korotcenkov, G., Porous silicon: from formation to application: formation and properties, Volume One. 2016: CRC Press. 34. Mekeef, Q.A., Characteristics of silicon Nanostructures produced by High power Lasers. 2010. https://doi.org/10.1201/b19342

[20] Dwivedi, P., Chauhan, N., Vivekananl. P., Scalable fabrication of prototype sensor for selective and sub-ppm level ethanol sensing based on TiO2 nanotubes decorated porous silicon. Sensors and Actuators B: Chemical, 2017. 249: p. 602-610. https://doi.org/10.1016/j.snb.2017.03.154

[21] Massad-Ivanir, N., et al., Porous silicon bragg reflector/carbon dot hybrids: synthesis, nanostructure, and optical properties. Frontiers in chemistry, 2018. 6: p. 574. https://doi.org/10.3389/fchem.2018.00574

[22] Zabotnov,S. V., Kurakina, D. A., Kashaev. F. V., A., Structural and optical properties of nanoparticles formed by laser ablation of porous silicon in liquids: Perspectives in biophotonics. Quantum Electronics, 2020. 50(1): p. 69. https://doi.org/10.1070/QEL17208

[23] Valerii Myndrul, Roman Viter, Maryna Savchuk, N., Porous silicon based photoluminescence immunosensor for rapid and highly-sensitive detection of Ochratoxin A. Biosensors and Bioelectronics, 2018. 102: p. 661-667. Reference 63. https://doi.org/10.1016/j.bios.2017.11.048

[24] Jabbar, A.A., A.M. Alwan, and A.J. Haider, Modifying and fine controlling of silver nanoparticle nucleation sites and SERS performance by double silicon etching process. Plasmonics, 2018. 13(4): p. 1171-1182. https://doi.org/10.1007/s11468-017-0618-x

[25] Hashim, D.A., A.M. Alwan, and M.F. Jawad, An investigation of structural properties of monometallic (Ag, Pd) and bimetallic (Ag& Pd) nanoparticles growth on macro porous silicon. 2018.

[26] Xiao, Q., Meng Gu, Hui Yang, Bing Li, Cu., Inward lithium-ion breathing of hierarchically porous silicon anodes. Nature communications, 2015. 6(1): p. 1-8. https://doi.org/10.1038/ncomms9844

[27] Adawyia, J.H., M.A. Alwan, and A.J. Allaa, Optimizing of porous silicon morphology for synthesis of silver nanoparticles. Microporous and Mesoporous Materials, 2016. 227: p. 152-160. https://doi.org/10.1016/j.micromeso.2016.02.035

[28] lwan, A.M., A.A. Yousif, and L.A. Wali, The growth of the silver nanoparticles on the mesoporous silicon and macroporous silicon: a comparative study. Indian Journal of Pure & Applied Physics (IJPAP), 2017. 55(11): p. 813-820.

[29] Bera, B., Porous silicon and its nanoparticles: a theoretical study. International Journal of Applied Nanotechnology, 2019. 5(1): p. 14-18p.

[30] Karthik, T., L. Martinez, and V. Agarwal, Porous silicon ZnO/SnO2 structures for CO2 detection. Journal of Alloys and Compounds, 2018. 731: p. 853-863. https://doi.org/10.1016/j.jallcom.2017.10.070

[31] Searson, P., J. Macaulay, and S. Prokes, The formation, morphology, and optical properties of porous silicon structures. Journal of the Electrochemical Society, 1992. 139(11): p. 3373. https://doi.org/10.1149/1.2069080

[32] Prušáková, L., et al. Quantum Size Effects in a Si: H Films Prepared by PECVD with Different Hydrogen-Diluted Silane. in Advances in Science and Technology. 2010. Trans Tech Publ. Reference 64. https://doi.org/10.4028/www.scientific.net/AST.74.137

[33] Salonen, J. and E. Mäkilä, Thermally carbonized porous silicon and its recent applications. Advanced Materials, 2018. 30(24): p. 1703819. https://doi.org/10.1002/adma.201703819

[34] FaragI, M., et al., Investigation of dielectric and optical properties of MgO thin films. Int. J. Adv. Eng., Technol. Comput. Sci., 2014. 1(1): p. 1-9.

[35] Hadi, H.A., , Abood T.H. , Mohi A.T. , Karim M.S.l., Impact of the etching time and current density on Capacitance-Voltage characteristics of P-type of porous silicon. World Scientific News, 2017. 67(2): p. 149-160.

[36] Sun, N., Zhou,D., Liu,W, Aikl., Sputtered titanium nitride films with finely tailored surface activity and

porosity for high performance on-chip microsupercapacitors. Journal of Power Sources, 2021. 489: p. 229406. https://doi.org/10.1016/j.jpowsour.2020.229406

[37] Zhanabaev, Z.Z., Turlykozhayeva, D. A .l., Current and capacitance hysteresis in porous semiconductor nanofilms. Physical Sciences and Technology, 2020. 7(3-4): p. 37-43. https://doi.org/10.26577/phst.2020.v7.i2.06

[38] Manakov, S., Ibraimov, M.K., Sagidolda,Ye., Detection of acetonitrile and chloroform using structures on the base of porous silicon. Eurasian Chemico-Technological Journal, 2019. 21(1): p. 89-93. https://doi.org/10.18321/ectj796

[39] Xu, J., et al., Preparation of porous silicon by electrochemical etching methods and its morphological and optical properties. Int. J. Electrochem. Sci, 2019. 14: p. 5188-5199. https://doi.org/10.20964/2019.06.10

[40] Škrabić, M., , Kosović, M.,Gotić,M., Lara., Near-infrared surface-enhanced Raman scattering on silver-coated porous silicon photonic crystals. Nanomaterials, 2019. 9(3): p. 421. https://doi.org/10.3390/nano9030421

[41] Roland, A., Dupuy,A., Machon,D., Fré., In-depth study of annealed porous silicon: Understand the morphological properties effect on negative LiB electrode performance. Electrochimica Acta, 2019. 323: p. 134758. https://doi.org/10.1016/j.electacta.2019.134758

[42] Juyal, S., Kumar,Y., Prasad,B., Stain etching of silicon with V2O5 and FeCl3: Effect of etching time on photoluminescence. Materials Today: Proceedings, 2020. 26: p. 3193-3196. Reference. https://doi.org/10.1016/j.matpr.2020.02.714

[43] R. Radzali1, M. Zakariah, A. Mahmood, A. Abd Rahim, Z. Hassan and Y. Yusof, The Effect of Ecthing Duration on Structural Properties of Porous Si Fabricated by a New Two-Steps Alternating Current Photo-Assisted Electrochemical Etching (ACPEC) Technique for MSM Photodetector. International Conference on Applied Physics and Engineering (ICAPE2016) AIP Conf. Proc. 1875, 020003-1-020003-10 (2017). https://doi.org/10.1063/1.4998357

[44] Y. Al-Douri, N. Badicd, and C. H. Voone, Etching time effect on optical properties of porous silicon for solar cells fabrication. Optik 147, 343-349 (2017). https://doi.org/10.1016/j.ijleo.2017.08.107

[45] K. Omar and K. Salman, Effects of Electrochemical Etching Time on the Performance of Porous Silicon Solar Cells on Crystalline N-Type (100) and (111). Journal of Nano Research 46, 45-56 (2017). https://doi.org/10.4028/www.scientific.net/JNanoR.46.45

[46] F. Mutlak, A. Ahmed, U. Nayef, Q. Al-zaidi, Improvement of absorption light of laser texturing on silicon surface for optoelectronic application. Optik 237, 16655 (2021). https://doi.org/10.1016/j.ijleo.2021.166755

[47] D. Jwied, U. Nayef, F. Mutlak, Synthesis of C: Se (core:shell) nanoparticles via laser ablation on porous silicon for photodetector application. Optik 231, 166493 (2021). https://doi.org/10.1016/j.ijleo.2021.166493

[48] T. Rashid, U. Nayef, M. Jabir, F. Mutlak, Study of optical and morphological properties for Au-ZnO nanocomposite prepared by Laser ablation in liquid, Journal of Physics: Conference Series. 1795(1), 012041 (2021). https://doi.org/10.1088/1742-6596/1795/1/012041

[49] U. M. Nayef, "Improve the efficiency of UV-detector by modifying the Si and porous silicon substrate with ZnS thin films," Optik, vol. 130, pp. 441-447, 2017.

[50] U. M. Nayef, "Fabrication and characterization of porous silicon for humidity sensor application.," Iraqi Journal of Physics, vol. 16, pp. 162-170, 2018.

[51] J. H. Song, M. J. Sailor, Quenching of photoluminescence from porous silicon by aromatic molecules. J. Am. Chem. Soc. 119, 7381 (1997). https://doi.org/10.1021/ja971209o

[52] U.M. Nayef, Improve the efciency of UV-detector by modifying the Si and porous silicon substrate with ZnS thin flms. Optik 130, 441 (2017). https://doi.org/10.1016/j.ijleo.2016.10.077

How to Cite

A. A. Urabe, U. M. Nayef, and R. . Kamel, “Influence Study of Etching Time for Porous Silicon on Morphological, Optical, Electrical and Spectral Responsivity Properties”, *Al-Mustansiriyah Journal of Science*, vol. 34, no. 2, pp. 113–120, Jun. 2023.